Sustainable Energy Technologies and Assessments 34 (2019) 35–42

Contents lists available at ScienceDirect

Sustainable Energy Technologies and Assessments

journal homepage: www.elsevier.com/locate/seta

Analysis and diagnosis of PEM fuel cell failure modes (flooding & drying) across the physical parameters of electrochemical impedance model: Using neural networks method

Slimane Laribi[a], Khaled Mammar[b], Youcef Sahli[a,c], Khaled Koussa[a]

[a] Unité de Recherche en Energies Renouvelables en Milieu Saharien, URERMS, Centre de Développement des Energies Renouvelables, CDER, 01000 ADRAR, Algeria
[b] Department of Electrical and Computer Engineering, University of Béchar, Bp 417, Algeria
[c] Department of Mechanical, Faculty of Technology, University of Batna 2, Algeria

ARTICLE INFO

Keywords:
Water management
Electrochemical impedance spectroscopy
PEMFC
Impedance model
Flooding
Drying

ABSTRACT

The objective of this work is to define and implement a method of artificial neural network to create an optimal impedance model of the proton exchange membrane fuel cell (PEMFC) which considers the electrochemistry and the mass transfer theory, which are used to analyze and diagnose PEM fuel cell failure modes (flooding & drying) across the physical parameters of the electrochemical impedance model. For this, we have based on the neural network technique for the calculation and estimation of various constituents parameters of this model. The Multi-Layer-Perceptron through back-propagation training algorithms shows satisfactory performance with the regard of parameter prediction. Furthermore, the neural network method applied to the impedance model is valid and valuable, which used to estimate the physical parameters of the electrochemical impedance model of the fuel cell (PEMFC) in both cases; flooding and drying of the fuel cell heart. The novelty of our work is summed up in the demonstration of the existence in a simple and uncomplicated way that allows the knowledge of the state of health of the PEMFC.

Introduction

For some years, the use of fossil fuels in conventional combustion engines leads to a significant emission of greenhouse gases. Declining fossil energy resources have led to finding other sources having the same properties of the hydrocarbons in terms of transport and storage. Hydrogen is the energy vector that is the best candidate characterized by a great caloric power to replace the fossil fuels [1,2]. Hydrogen does not exist in its free molecular form, but only in chemical compounds, such as water and hydrocarbons. In addition to its energy vector function, its storable character can satisfy the energy consumer requirements. Among its uses, hydrogen is adopted as fuel in the PEM fuel cells, these cells are not a recent technology, and their operating principle was discovered by Sir William Grove in 1839. Actually, fuel cell gives a considerable contribution to the renewable energy development and environmental conservation.

Several fuel cell types exist that are classified according to the operating temperature, the nature of the electrolyte and the conductor type.

Among these existing families, we are interested in the cells to have a polymer membrane, an exchange of protons and a low operating temperature, these fuel cells are used in the Gemini space program by NASA in the sixties of last century [1].

Currently, PEMFC is considered the best fuel cell type to use in the transport sector. Among its advantages, the dynamics compared to other fuel cell types, an easy installation in transport means without the use of the thermal insulation and an operating temperature very low (40–100 °C) compared to other fuel cell types [3,4]. PEMFC consists of a cathode and an anode that are separated by a membrane as an electrolyte that permits the transformation of the chemical energy into electrical energy [5].

In the fuel cells that use the hydrogen as a fuel, the conversion of the chemical energy into electrical energy is realized simultaneously along with the heat and water production. In redox chemical reaction, the hydrogen combines with oxygen to produce the water, electrical and thermal energies according to the following equation [3,4,6]:

$$H_2 + 1/2O_2 \rightarrow H_2O + Heat + \text{electrical energy} \quad (1)$$

At the anode, the hydrogen decomposes into protons and electrons. The impermeable membrane to the gases passed only the protons. The electrons are conducted from the anodic part to the cathodic part through the external circuit. At the cathode, the oxygen is combined

E-mail address: laribi.slimane@urerms.dz (S. Laribi).

https://doi.org/10.1016/j.seta.2019.04.004
Received 19 September 2017; Received in revised form 1 March 2019; Accepted 17 April 2019

Nomenclature

C	Oxygen concentration in the cathode active layer (mol m^{-3})
δ	Diffusion layer width (m)
D	Diffusion coefficient ($m^2 s^{-1}$)
F	Faraday constant (A s mol^{-1})
N	Electron numbers
R	Perfect gas constant (J $mol^{-1} K^{-1}$)
R_d	Diffusion related resistance (Ω)
R_m	Electrolyte ohmic resistance (Ω)
R_p	Polarisation resistance (Ω)
R_{int}	Internal resistors measured at high frequency (Ω)
R_{pol}	Biasing resistor measured at low frequency (Ω)
Q	CPE parameter or double layer capacitance at the electrode/electrolyte interface (S s^{α})
S	Active area (m^2)
T	Temperature (K)
t	Time (sec)
Z_T	Fuel cell impedance (Ω)
Z_{CPE}	CPE impedance (Ω)
Z_w	Warburg impedance (Ω)
τ_d	Diffusion time constant (s)
α	CPE power
ω	Pulsation (rad s^{-1})
j	Imaginary number

Abbreviations

RH	Relative humidity (%)
NNT	Neural Network
PEMFC	Proton Exchange Membrane Fuel Cell
PEM	Proton Exchange Membrane
EIS	Electrochemical impedance spectroscopy
CPE	Constant Phase Elements

with the electrons and protons to produce the water and electrical and thermal energies [7]. The global reaction (Eq. (1)) can be decomposed in both half-reactions (Eqs. (2) and (3)) which produced respectively in the anode and cathode Fig. 1.

$$H_2 \rightarrow 2H^+ + 2e^- \text{Anode} \quad (2)$$

$$O_2 + 4H^+ + 4e^- \rightarrow H_2O \text{ Cathode} \quad (3)$$

The water production is one of the electrochemical reaction results, this affirmed that water management is very essential to ensure an ideal operation of the PEMFC. This is any of the most important aspects of the fuel cell operation since the membrane must be saturated with water to ensure the movement of H^+ [8]. In addition, a water lacks can lead to a membrane drying and conduct to the PEMFC destruction. Conversely, a water excess leads to a decreasing of the reactive species transport and causes the cell yield reduction. Logically, the hydration diagnostic and control are very important to ensure the best hydration of the membrane without any risk of engorgement or saturation of the cell [9,10].

Different methodologies have been proposed to study and diagnose water management in PEMFCs, such as methods the analytical, physical, empirical and artificial intelligence …etc. [11–16]. In addition, the impedance measurements are widely used techniques in the diagnosis of the PEMFC water management problems [9,19,20]. Fouquet et al [9] have treated the hydration monitoring using an approach based on the spectroscopic impedance measurement (EIS) and the Randles model enhanced by a CPE.

Futter et al. [21] have developed a 2D theoretical and physical model based continuum-level modeling to analyze and diagnose the water management impact on PEMFC performance using a new NEOPARD-X digital frame. The impedance spectroscopic and I-V curves are used to validate this model. Tant et al. [22] have presented a study to identify and characterize the PEM fuel cell flooding using impedance spectroscopy measurements (EIS) associated to the physical-based model. The detection Gas Diffusion Layers flooding of PEMCF has been done by a new algorithm to determine the parameters change during the flooding operation. Hernandez et al. [23] developed a new model of

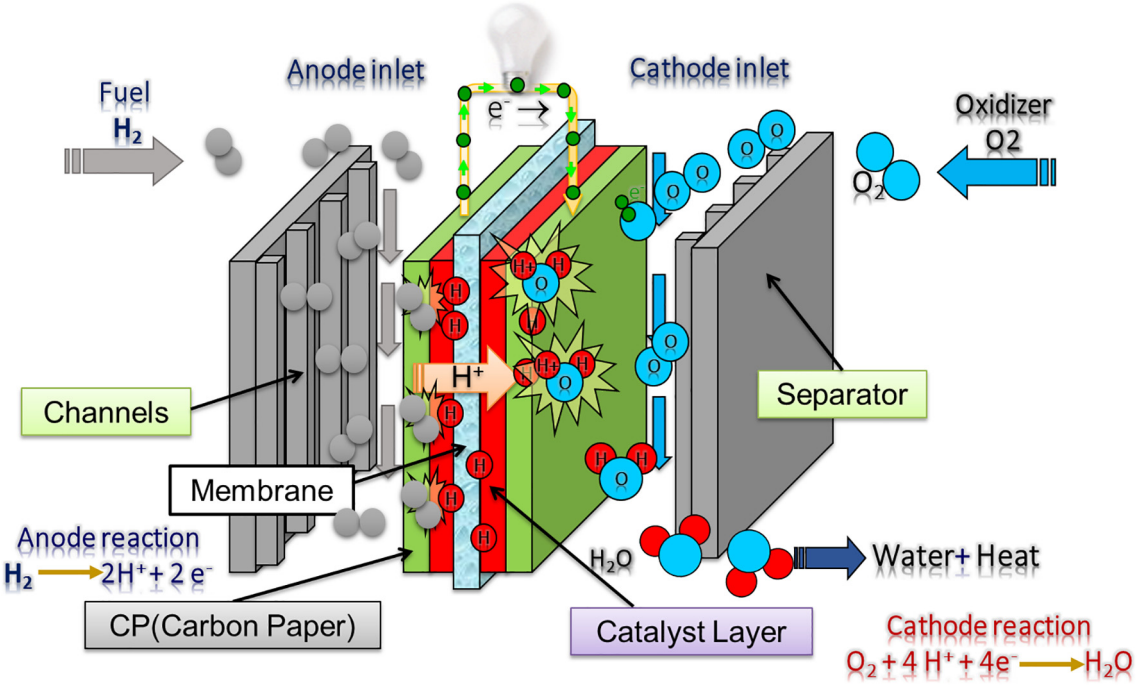

Fig. 1. Basic PEM Fuel Cell operation.

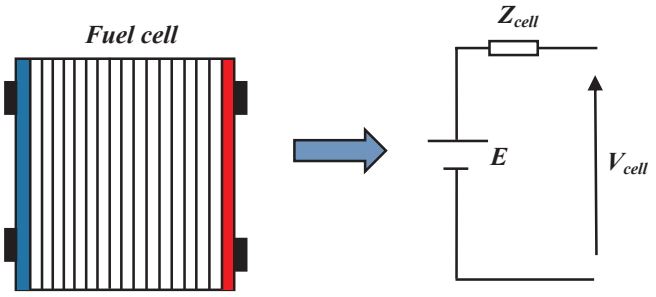

Fig. 2. Representation of a fuel cell by a voltage source associated with its electrical impedance.

PEMFC based on an electrical equivalent circuit to be used in diagnostic algorithm, taking into account three types of technical failures of PEMFC: flooded, drying and membrane degradation. PEMFC stacks hydration state is clearly shown by the resistance flow, which is insufficient to determine the original of the failure. Roy et al. [24] proposed a new diagnosis experimental technique using EIS impedance measurement coupled with a measurement model-based stochastic errors analysis to detect the appearance of PEMFC flooding and drying.

The control and diagnosis of PEMC defects require knowledge of a number of internal parameters during fuel cell operation, but due to insufficient adequate instruments for monitoring tasks makes monitoring very complicated. For PEMFCs destined for the transportation applications, the fuel cell manufacturers aim to reduce the number of used equipment in monitoring and control. Black box models that recognize a minimum of inputs variables used to evaluate the output parameter values are highly desirable. These models are recognized by their speed, precise and easily, compared to the analytical, physical and empirical models. The neural network is one of the techniques used to identify the black boxes behavior. Among the advantages of this artificial intelligence method, identify and approximate the nonlinear functions without recognizing the details of physical processes.

Several works have been used the neural network method in the diagnosis of PEMFCs. Kim et al. [25] have diagnosed the health state of 20 PEMFCs cells, using a Hamming neural network and the PEMFC measured electrical performance (voltage, current), which are used as training and validation data, in order to create a PEMFC hamming neural network able to determine the suitable parameters of an equivalent circuit model, from which the PEMFC failure can be detected and separated. Silva et al. [26] have been proposed a new method based on Adaptive Neuro-Fuzzy Inference Systems to predict the output voltage reduction caused by the PEMFC nominal degradation conditions during long term operation test. Shao et al. [27] have been used an efficient technologies for fault diagnosis in PEMFC systems. This proposed method based on ANN ensemble method (BP-ANN) and the PEMFC dynamic model, from which the PEMFC fault types can be detected with an accuracy varied between 75.24% and 85.62%.The parameters that are characterized these faults were simulated as a function of time: current ,voltage, air flow, temperature, and pressures H_2,O_2. Yousfi et al. [28] presented a method for diagnosing the drying and flooding problems of the PEMFCs based on the comparison between two residues of the real system outputs and the NNT model outputs (pressure drop and stack voltage) to detect the PEMFC health state.

In the continuation of our studies that already published in fuel cells [18,29–38], this work presents a new diagnostic procedure for the water management problems (drying and flooding) in the PEMFC to detect and identify the fuel cell health state based on the neural network methodology. The NNT inputs parameters are: the operating time and the relative humidity; and the NNT outputs of physical impedance parameters of the Randles model ameliorated by a CPE are: the membrane resistance, the polarization resistance, the double layer capacity at the electrode/electrolyte interface, the species diffusion resistance and the time constant of the charges diffusion. The PEMFC health state can be determined simply by one estimated physical parameters of the proposed model that gave a better PEMFC membrane resistivity, with less parameters requirements. Although, each of its parameters can show the operation state of the cell using only the oxidizer relative humidity and the operating time. The obtained results are validated with the experimental results that have been taken from the literature review. In addition, according to the present study and the investigated results, the proposed method is simple, uncomplicated, speed, precise, and easily allows to knowledge the PEMFC health state.

Impedance model formulation

The fuel cell simplest representation in the form of an electric model consists in putting a direct voltage source in series with an electrical impedance. Fig. 2. In this paper, we will proceed to the determination of this Z_{cell} impedance.

PEMFC impedance model

Since 1947, the model developed by Randles for the representation of multi-type phenomena redox reaction produced between the electrodes and the membrane is supposed to be valid; it is composed of an electrolyte resistance in series with a circuit composed of a double-layer capacitor in parallel with a serial charge transfer resistance with a Warburg impedance.

In 2006, Fouquet et al. [9] have improved the Randles model for using in the PEMFC control domain, this enhanced consists essentially of a change of the double layer capacity by a CPE Fig. 3.

Fouquet et al. [9] improvement render the circuit capable to capture all the action with very little error compared with Randles model.

According to the Butler-Volmer equation and diffusion second law of Fick, the impedance diffusion expression for a finite length diffusion layer is given by the following equation [9,18,38,39]:

$$Z_w(j\omega) = \frac{RT\delta}{n^2F^2SCD}\frac{\tanh\sqrt{j\omega(\delta^2/D)}}{\sqrt{j\omega(\delta^2/D)}} \quad (4)$$

Eq. (4) can be written as follows [9,17,18,38,39]:

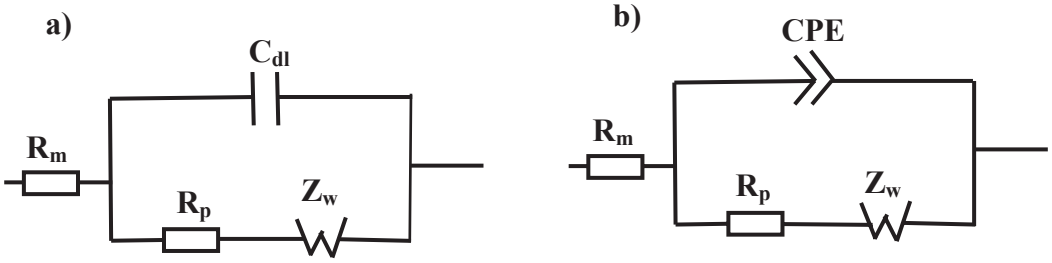

Fig. 3. Equivalent circuit. a) Randles model, b) Fouquet improvement [9,18,30].

$$Z_w(j\omega) = R_d \frac{\tanh\sqrt{j\omega(\delta^2/D)}}{\sqrt{j\omega(\delta^2/D)}} \quad (5)$$

where the diffusion time constant (τ_d) is given by the ratio of the diffusion layer and diffusion coefficient ($\tau_d = \delta^2/D$) and the diffusion resistance (R_d) is given by the Eq. (6) [9,18,38].

$$R_d = \frac{RT\delta}{n^2F^2SCD} \quad (6)$$

The PEMFC impedance model consists of both impedance at each electrode (anode and cathode). These impedances are placed in series with an internal resistance bound to the membrane.

According to Fouquet et al. [9], the limiting of the reaction rate is linked to the oxygen reduction at the cathodic part and the contribution of the anode impedance is neglected in the global cell impedance. The PEMFC equivalent circuit is represented in Fig. 4. The fuel cell global impedance is given by the Eq. (7).

$$Z_T(j\omega) = R_m + \frac{1}{Z_{CPE} + (1/(R_P + Z_w))} \quad (7)$$

The CPE impedance is defined by [9,18,40,41]:

$$Z_{CPE}(j\omega) = \frac{1}{Q(j\omega)^{\alpha}} \quad (8)$$

The polarization resistance (R_P) characterizes the charge transfer phenomena at the electrodes.

With a value of α usually varies between 0.5 and 1.

For the identification of the model parameters, we used a nonlinear method, which is based on the least square method, to identify all the parameters of the cell Randles improved by CPE.

The proposed algorithm principle is founded on the nonlinear function square minimization while finding the unknown variable best values (i.e. model parameters) starting from their given initial values in the table [9,18,41] for the cell flooding and drying (RH = 10% and RH = 100%).

Modelling by the impedance of pile PEMFC with artificial neural network

The NNT principle is based on the function approximations. In this study, we proceed to use of an NNT of type feed-forward with a supervised training to realize an NNT that based on these steps: the NNT block construction, learning, defect classifications and neuron network test.

The used NNT in this work consists of three layers. The first layer represents the input layer, the second layer represents the hidden layer and the third layer represents the output layer. In the network, each neuron is linked to the next layer neurons as shown in Fig. 4a.

The sigmoid function is used in the hidden layer as a transfer function; it is given by the following equation [18,42]:

$$f(u) = \frac{1}{1 + e^{-(d.u)}} \quad (9)$$

With d is the curve steepness. The hidden layer input is given by the following equation [41]:

$$u = \sum_{j=1}^{n} (w_{ij}x_i + b_i) \quad (10)$$

where x_i is the input signal, w_{ij} represent the synaptic weights of the neuron j, whose function is to simulate the synaptic weights with weight respectively associated to each neuron input. These weights weigh inputs and can be modified in the learning and b_i represent the bias input that takes the value -1 or $+1$.

For an output layer function linear, the equation that represents the network model is given by [18,41]:

$$y_k u = \sum_{j=1}^{N} (w_{ij}^0 u_i + b_i) = \sum_{j=1}^{N} w_{ij}^0 f\left(\sum_{j=1}^{N} (w_{ij}x_i + b_i)\right) \quad (11)$$

where y_k represents the output signal from kth output neuron, $w^0{}_{ki}$ represents the weight of ith output u_i to the kth neuron in the output layer and u_i is the activation value of the jth neuron in the ith layer.

In this work, the values of neural network bias and the weight are updated according to the dynamic gradient descent algorithm [42,43].

The NNT input layer part is composed of two neurons, the first input neuron is bound to the operation time and the second input neuron is bound to the relative humidity. The hidden layer is constituted of two under-layers of 20 and 10 neurons for the first under-layer and the second under-layer respectively. The output layer is composed of 5 neurons. To proceed to impedance physical parameter simulation, we

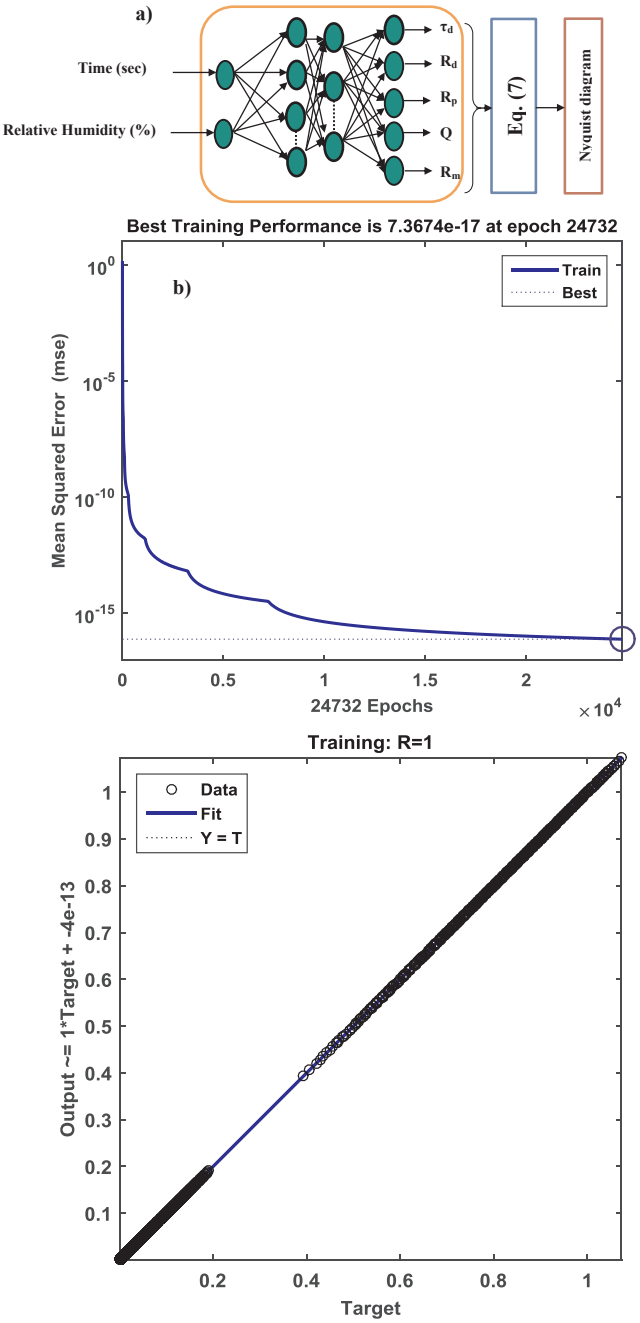

Fig. 4. PEMFC impedance model. a) NNT architecture, b) Training mean squared error, c) Linear regression coefficient.

completed the MATLAB code development which based on the presented model by using the Neural Networks Toolbox of MATLAB. The “tansig" (hyperbolic tangent sigmoid transfer) function is used to estimate the hidden layer parameters and the ”purelin" (linear transfer) function is used to estimate the output layer parameters.

Once all the parameters of our neuron network (the database, the architect, activation function, the number of necessary iterations …etc.) are defined, we pass to the learning phase, this phase represents an iterative procedure of estimating the parameters of network neurons in order for the latter to fulfil its task [42,43]. When the learning phase is completed, the network must be able to make the right associations for input vectors that it has not learned. The supervised learning is done by the back-propagation algorithm to adapt the weights, the thresholds (biases) to satisfy an optimization criterion. Consequently; a neural network is generated which represents the impedance physics parameter estimator. The values to be predicted are the Randles model physical parameters expands (R_m,Q,R_p,R_d,τ_d) and the input values are: relative humidity (RH) and operating time t (sec). For each value of time and relative humidity, the model is able to easily give information on the evolution of the physical parameters of the PEMFC impedance.

The NNT training performance in terms of Mean Squared Error (MSE) and the iteration number (EPOCHS) is presented in Fig. 4b.

Fig. 4c shows the relationship between the results obtained by the NNT model and the results obtained experimentally by Fouquet et al. [9]. The Linear regression coefficient (Pearson correlation coefficient) is equal to one (1) since the mean squared error is $7.3674{\cdot}10^{-17}$.

Model test and validation

For realizing the impedance NNT learning, we have proceeded to use the values of parameters that are shown by Table 1, for both studied cases: flooding and drying of the fuel cell heart [9]. In the learning, the least square method is used for parameters identifying of Randles model enhanced by Fouquet.

After the realization of the impedance NNT learning, we have proceeded to the test and validation of the results obtained by the simulation based on a comparison of the simulation results with the experimental results of Fouquet et al. [9] for both cases: flooding and drying of the fuel cell heart.

In the fuel cell heart drying case, two validation tests are shown in Fig. 5a; the inputs parameters of the first test are taken from Fig. 11 that is presented by Fouquet et al. [9], where the relative humidity and the time are respectively RH = 15% and 180 sec and the frequency range is 0.1 Hz to 1 kHz. The inputs parameters used in the second test are also taken from Fig. 11 of the reference [9] where the relative humidity and the time are respectively RH = 20% and 1600 sec and the frequency range is the same of the first teste (0.1 Hz to 1 kHz).

In the fuel cell heart flooding case, two validation tests are shown in Fig. 5b; the inputs parameters of the first test are taken from Fig. 9 that is presented by Fouquet et al. [9], where the relative humidity and the time are respectively RH = 100% and 500 s and the frequency range is 0.1 Hz to 1 kHz. The inputs parameters used in the second test are also taken from Fig. 9 of the reference [9] where the relative humidity and the time are respectively RH = 100% and 1600 s and the frequency range is the same used in the first test (0.1 Hz to 1 kHz).

In a drying state of the PEMFC, the beginning of the faradic arc (R_{int}) and the end of the transport arc (R_{pol}) are gradually shifting according to the time. Fig. 5a. For a flooded state of the fuel cell, the beginning of the faradic arc (R_{int}) remains fixed and the end of the transport arc (R_{pol}) develops progressively with the time. Fig. 5b. The rays of both arcs (faradic and transport) develop rapidly as a function of the time (500–1600 s) in flooding case of the PEMFC compared to the drying case of the fuel cell (180–1600 s) Fig. 5.

From Fig. 5, the comparison between numerical and experimental results of each test shows that the used model is really reliable.

Results and discussion

To process the PEMFC NNT impedance model simulation in a time variation of (600 sec to 3600 sec) at drying conditions, we give in every simulation; the air supply relative humidity and time as model inputs.

After the NNT impedance model simulation, an estimate of the ameliorate Randles model parameters (R_m, Q, R_p, R_d, τ_d) is obtained to use in Z_T ($j\omega$) function calculation and finally plotted by “Nyquist plot MATLAB”.

The impedance Nyquist diagram spectra presented in Fig. 6a and b show the drying and flooding conditions of the PEMFC respectively. For Fig. 6a, it is clearly visible at the high frequency that the impedance Nyquist diagram spectra (faradic arcs) move progressively as a function of the operating time towards the right side of the real axis, whereas, they are fixed at the same point in the flooding case presented in Fig. 6b. The progressive shifting of the impedance Nyquist diagram spectra at higher frequency is due to the increase of the membrane internal resistance of the PEMFC (R_{int}). On the other hand, the absence of this shift in the impedance Nyquist diagram spectra at the high frequency in the flooding case is logically the result of the non-variation of the membrane internal resistance value.

At low frequency, the end of the impedance Nyquist diagram spectra (transport arcs) develops progressively as a function of the operating time in both cases (flooding and drying). This progressively developing is due to the increase of the polarization resistance of the PEMFC (R_{pol}). In addition, in the flooding case, the faradic and transport arcs develop rapidly as a function of time compared to the drying case.

The relative humidity of air supply has a direct effect on flooding and drying of PEMFC, which is clearly presented in the impedance spectra of the Nyquist plot. Fig. 7. We find that the surfaces of the impedance Nyquist diagram spectra are increased and decrease according to the operating time and relative humidity.

For monitoring and diagnosis of the health state of the PEMFC in the case of drying or flooding of the fuel cell heart, we followed the physical parameter evolution (R_m, Q, R_p, R_d, τ_d).

Fig. 8 shows that the membrane ohmic resistance value increases with the operating time when the air supply relative humidity decreases from 100% to 10%. The main reason leads to increase the membrane resistance is the membrane ionic conductivity, which is linked directly with water content. When the air supply relative humidity increases, the membrane water content increases, also, the membrane ionic conductivity increases and the internal resistors measured at high frequency decreases and the resistance measured at low frequency increases.

These resultant changes are directly linked to the molar variation of water flow injected in the air. In addition, the air supply relative humidity has an impact on the proton mobility at the high frequency.

Fig. 9 presents the variation of the double layer capacitance at the electrode /membrane interface. The gradual decrease in the values of the double layer capacitance (Q) according to the operating time is clearly remarkable in Fig. 9. In addition, it decreases when the air supply relative humidity decreases.

Fig. 10 shows the ohmic resistance polarization behavior. The ohmic resistance polarization increases according to the operating time if the air supply relative humidity increases. In other words, the air

Table 1
Parameters of the model during the fuel cell flooding and drying [9,18].

Time (s)	RH (%)	R_m (ohm)	Q (S s^{α})	R_p (ohm)	R_d (ohm)	τ_d (s)	U(V)
500	10	0.00512	0.952	0.0099	0.0051	0.1155	4.06
3700	10	0.0088	0.62	0.013	0.0101	0.1835	3.35
500	100	0.00398	1.109	0.008	0.0034	0.0872	4.18
3700	100	0.00416	0.936	0.0163	0.0312	0.0947	3.3

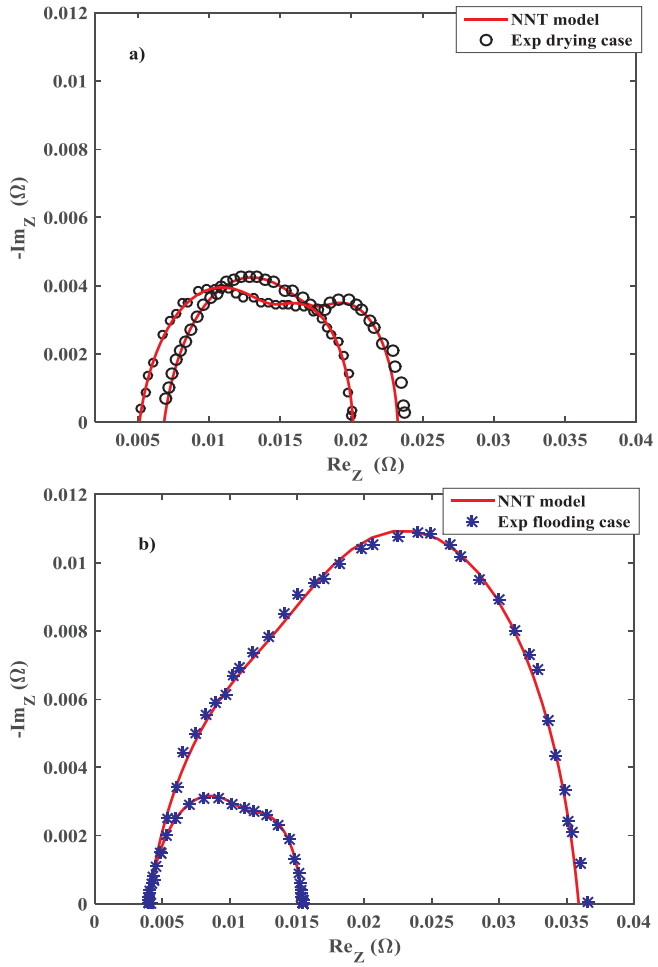

Fig. 5. Model validation for the PEMFC flooding and drying cases.

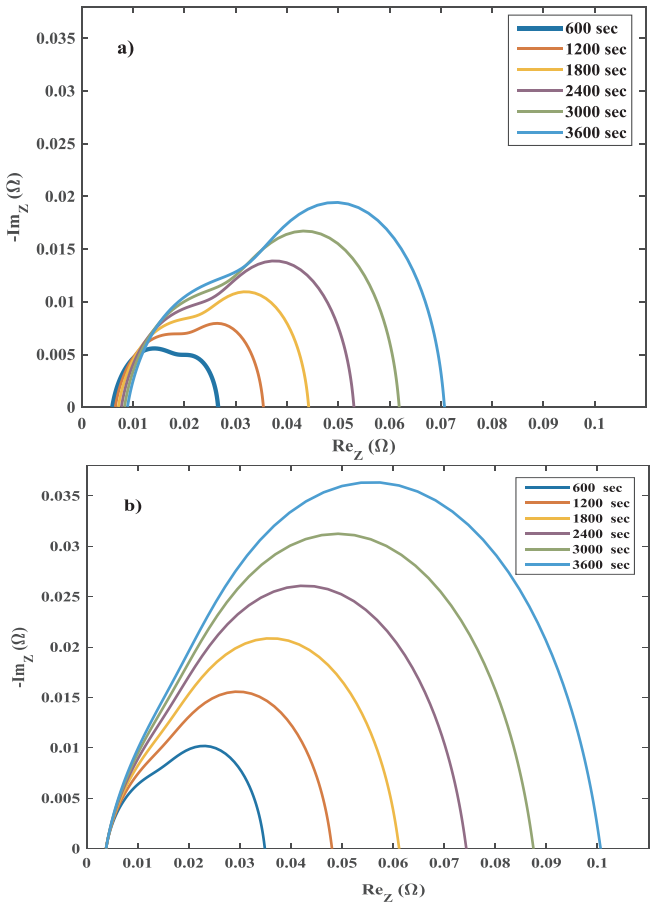

Fig. 6. PEMFC Nyquist diagram with different operating times. a) Drying case, b) Flooding case.

supply relative humidity increasing provokes the increasing of the membrane water content. Consequently, the membrane ionic conductivity increase which conducts to a decrease in the charge transfer resistance.

Figs. 11 and 12 show that value the diffusion time constant and the diffusion ohmic resistance change inversely. The diffusion ohmic resistance value increases according to the operating time if the air supply relative humidity increases from 10% to 100%. Also, the diffusion time constant value decreases in the same condition, in other words, when the diffusion ohmic resistance of species in GDL increases, the diffusion time constant of species decreases. This corresponds to the results obtained by the references [9,18,30,44].

Conclusion

In this paper, we based on the neural network technique for creating the optimal model of PEM fuel cell toward diagnosing and analyze the impact of the air supply relative humidity on the water management in its core. This technique represented by an equivalent electrical circuit called Randles with a CPE for diagnosis of the proton exchange membrane fuel cell (PEMFC) behavior in both cases: flooding and drying of the cell heart. This model improved by the CPE was judged to be an accurate model relatively in the fuel cell's electrical response over the large operating ranges. This new approach has enabled us to identify the parameter set composed of five alternatives that exhibited a high sensitivity to the PEMFC diagnostic.

The hydration monitoring status of the PEMFC is demonstrated very robust and reliable under the diagnosis of the impedance parameters

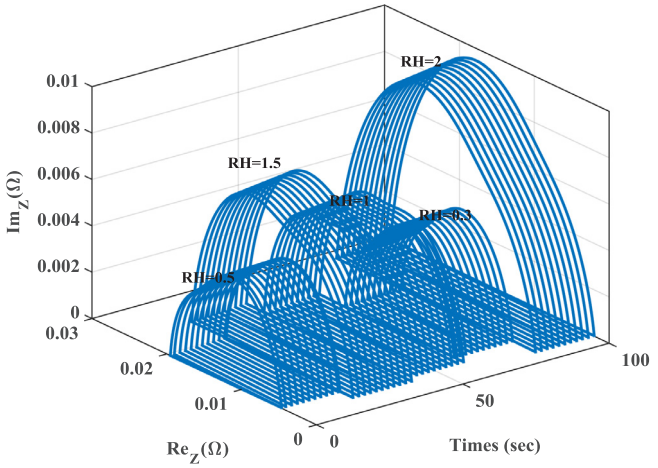

Fig. 7. PEMFC Nyquist diagram with different relative humidities.

(R_m, Q, R_p, R_d, τ_d).

The effects analysis of the decrease and increase recorded in the air supply relative humidity values on the water management shows that:

- When the air supply relative humidity at the cathode increases the water content increased to the cathode gradually, which also causes clear decreases in the ohmic resistance of the membrane and the diffusion time constant, and a remarkable augmentation on the ohmic resistance polarization, the diffusion resistance and the double layer capacitance electrode/membrane interfaces.

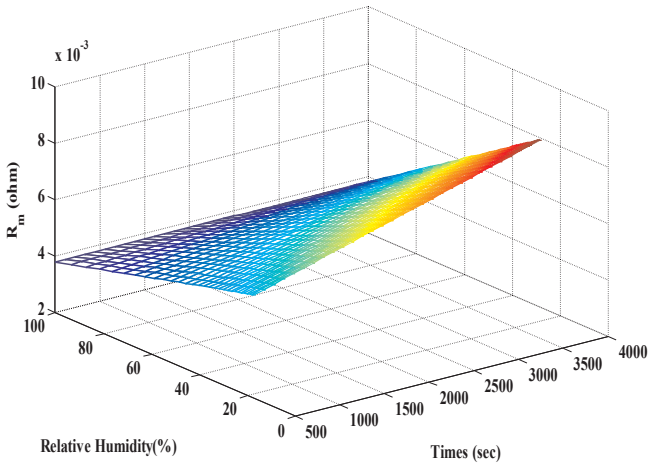

Fig. 8. Membrane ohmic resistance R_m.

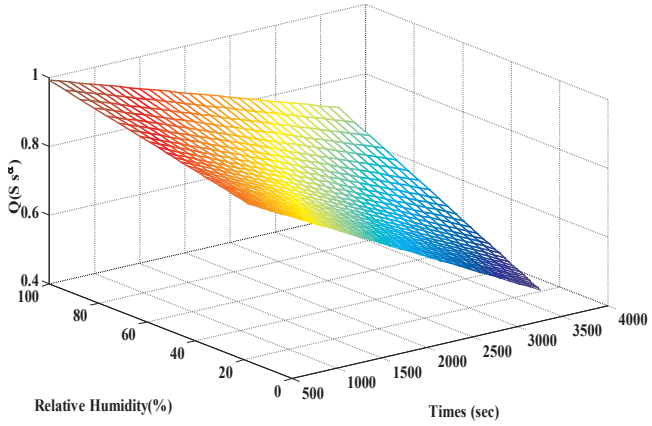

Fig. 9. Double layer capacitance at the electrode/ electrolyte interface Q.

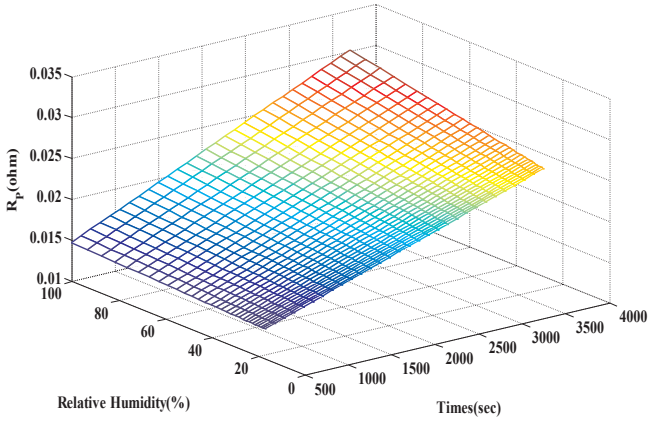

Fig. 10. Polarization resistance R_p.

- When the oxidant relative humidity decreases at the cathode, the water content decreases in parallel, which leads to a logic increases of the ohmic resistance of the membrane and the diffusion time constant, and the decreases evident in the ohmic resistance polarization, the diffusion resistance, and the double layer capacitance electrode/membrane interfaces.
- When the air supply relative humidity rises, the surfaces of the impedance Nyquist diagram spectra are increased according to the operating time. If the case of a decreasing of the air supply relative humidity, the opposite is obtained.

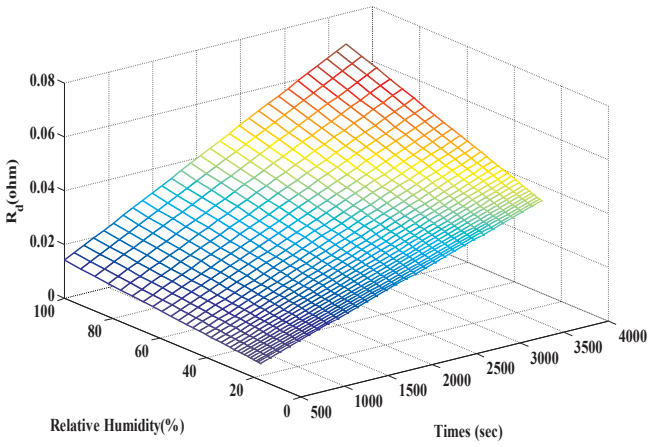

Fig. 11. Diffusion resistance R_d.

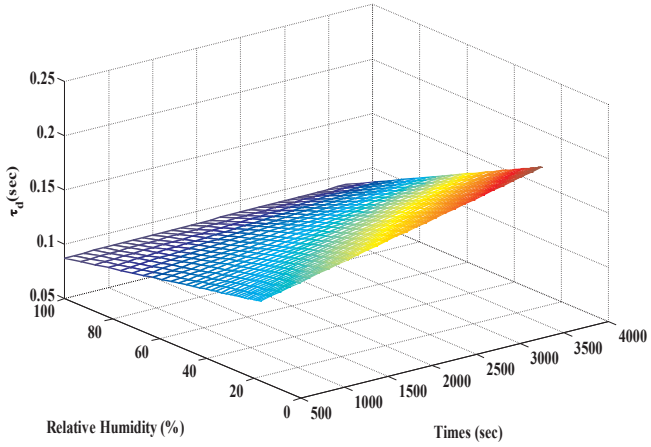

Fig. 12. Diffusion time constant τ_d

References

[1] Rezaei Niya SM, Hoorfar M. Study of proton exchange membrane fuel cells using electrochemical impedance spectroscopy technique – a review. J Power Sources 2013;240:281–93.

[2] Benmouna A, Becherif M, Depernet D, Ebrahim MA. Novel energy management technique for hybrid electric vehicle via interconnection and damping assignment passivity based control. Renew Energy 2018;119:116–28.

[3] Corrêa JM, Member S, Farret FA, Canha LN, Simões MG, Member S. An electrochemical-based fuel-cell model suitable for electrical engineering automation approach. IEEE Trans Indust Electr 2004;51:1103–12.

[4] Outeiro MT, Chibante R, Carvalho AS, De Almeida AT. A parameter optimized model of a Proton Exchange Membrane fuel cell including temperature effects. J Power Sources 2008;185:952–60.

[5] Friede W, Rael S, Davat B. Mathematical model and characterization of the transient behavior of a PEM fuel cell. IEEE Trans Power Electron 2004;19:1234–41.

[6] Mousa G, Golnaraghi F, Devaal J, Young A. Detecting proton exchange membrane fuel cell hydrogen leak using electrochemical impedance spectroscopy method. J Power Sources 2014;246:110–6.

[7] Candusso D, Hissel D, Hernandez A, Aslanides A. A review on PEM voltage degradation associated with water management: impacts, influent factors and characterization. J Power Sources 2008;183:260–74.

[8] Ji M, Wei Z. A review of water management in polymer electrolyte membrane fuel cells. Energies 2009;2:1057–106.

[9] Fouquet N, Doulet C, Nouillant C, Dauphin-Tanguy G, Ould-Bouamama B. Model based PEM fuel cell state-of-health monitoring via ac impedance measurements. J Power Sources 2006;159:905–13.

[10] Boulon L, Agbossou K, Hissel D, Hernandez A, Bouscayrol A, Sicard P, et al. Energy management of a fuel cell system: influence of the air supply control on the water issues. IEEE Int Symp Ind Electron 2010:161–6.

[11] Candusso D, Steiner NY, Hissel D, Moc P. Diagnosis of polymer electrolyte fuel cells failure modes (flooding & drying out) by neural networks modeling. Int J Hydrogen Energy 2010;36:3067–75.

[12] Yang D, Ma J, Xu L, Wu M, Wang H. The effect of nitrogen oxides in air on the performance of proton exchange membrane fuel cell. Electrochim Acta 2006;51:4039–44.

[13] Zheng Z, Petrone R, Péra MC, Hissel D, Becherif M, Pianese C, et al. A review on

non-model based diagnosis methodologies for PEM fuel cell stacks and systems. Int J Hydrogen Energy 2013;38:8914–26.
[14] Petrone R, Zheng Z, Hissel D, Péra MC, Pianese C, Sorrentino M, et al. A review on model-based diagnosis methodologies for PEMFCs. Int J Hydrogen Energy 2013;38:7077–91. https://doi.org/10.1016/j.ijhydene.2013.03.106.
[15] Pant LM, Yang Z, Perry ML, Weber AZ. Development of a simple and rapid diagnostic method for polymer-electrolyte fuel cells. J Electrochem Soc 2018;165:F3007–14.
[16] Pei P, Li Y, Xu H, Wu Z. A review on water fault diagnosis of PEMFC associated with the pressure drop. Appl Energy 2016;173:366–85.
[17] Taleb MA, Béthoux O, Godoy E. Identification of a PEMFC fractional order model. Int J Hydrogen Energy 2017;42:1499–509. https://doi.org/10.1016/j.ijhydene.2016.07.056.
[18] Laribi S, Mammar K, Hamouda M, Sahli Y. Impedance model for diagnosis of water management in fuel cells using artificial neural networks methodology. Int J Hydrogen Energy 2016;41.
[19] Génevé T, Régnier J, Turpin C. Fuel cell flooding diagnosis based on time-constant spectrum analysis. Int J Hydrogen Energy 2016;41:516–23.
[20] Asghari S, Mokmeli A, Samavati M. Study of PEM fuel cell performance by electrochemical impedance spectroscopy. Int J Hydrogen Energy 2010;35:9283–90.
[21] Futter GA, Gazdzicki P, Friedrich KA, Latz A, Jahnke T. Physical modeling of polymer-electrolyte membrane fuel cells: understanding water management and impedance spectra. J Power Sources 2018;391:148–61.
[22] Tant S, Rosini S, Thivel P-X, Druart F, Rakotondrainibe A, Geneston T, et al. An algorithm for diagnosis of proton exchange membrane fuel cells by electrochemical impedance spectroscopy. Electrochim Acta 2014;135:368–79.
[23] Hernandez A, Hissel D, Outbib R. Modeling and fault diagnosis of a polymer electrolyte fuel cell using electrical equivalent analysis. IEEE Trans Energy Convers 2010;25:148–60.
[24] Roy SK, Orazem ME. Analysis of flooding as a stochastic process in polymer electrolyte membrane (PEM) fuel cells by impedance techniques. J Power Sources 2008;184:212–9.
[25] Kim J, Lee I, Tak Y, Cho BH. State-of-health diagnosis based on hamming neural network using output voltage pattern recognition for a PEM fuel cell. Int J Hydrogen Energy 2011;37:4280–9.
[26] Silva RE, Gouriveau R, Jemeı S, Hissel D, Boulon L, Agbossou K, et al. Proton exchange membrane fuel cell degradation prediction based on Adaptive Neuro-Fuzzy Inference Systems. Int J Hydrogen Energy 2014;9.
[27] Shao M, Zhu X-J, Cao H-F, Shen H-F. An artificial neural network ensemble method for fault diagnosis of proton exchange membrane fuel cell system. Energy 2014;67:268–75.
[28] Yousfi Steiner N, Hissel D, Moçtéguy P, Candusso D. Diagnosis of polymer electrolyte fuel cells failure modes (flooding & drying out) by neural networks modeling. Int J Hydrogen Energy 2011;36:3067–75.
[29] Mammar K, Laribi S. Application of adaptive neuro-fuzzy inference system techniques to predict water activity in proton exchange membrane fuel cell. J Electrochem Energy Convers Storage 2018;15:041009.
[30] Laribi S, Mammar K, Sahli Y, Koussa K. Air supply temperature impact on the PEMFC impedance. J Energy Storage 2018:17.
[31] Sahli Y, Zitouni B, Ben-Moussa H. Solid oxide fuel cell thermodynamic study. Çankaya Univ J Sci Eng 2017;14:134–51.
[32] Sahli Y, Zitouni B, Ben-moussa H. Thermodynamic optimization of the solid oxyde fuel cell electric power. UPB Sci Bull Ser B Chem Mater Sci 2018;80:159–70.
[33] Monsaf Tamerabet, Moussa Hocine Ben, Youcef Sahli, Abdallah Mohammedi. Unsteady three-dimensional numerical study of mass transfer in PEM fuel cell with spiral flow field. Int J Hydrogen Energy 2017;42:1237–51. https://doi.org/10.1016/j.ijhydene.2016.12.084.
[34] Sahli Y, Zitouni B, Ben-Moussa H. Optimization study of the produced electric power by SOFCs. Int J Hydrogen 2018:43. https://doi.org/10.1016/j.ijhydene.2018.08.162.
[35] Sahli Y, Zitouni B, Ben Moussa H, Abdenebi H. Three-Dimensional Numerical Study of the Heat Transfer on the Planar Solid Oxide Fuel Cell: Joule's Effect. In: Dincer I, Ozgur Colpan C, Kizilkan O, Akif Ezan M, editors. Progress in clean energy volume I: Analysis and Modeling. Switzerland: Springer; 2015. p. 449–61. 10.1007/978-3-319-16709-1_32.
[36] Abdenebi H, Zitouni B, Ben-Moussa H, Haddad D, Zitouni H, Sahli Y. Inlet Methane Temperature Effect at a Planar SOFC Thermal Field Under Direct Internal Reforming Condition. In: Dincer I, Ozgur Colpan C, Kizilkan O, Akif Ezan M, editors. Progress in clean energy volume II: Novel Systems and Applications Switzerland: Springer; 2015. p. 567–81. https://doi.org/10.1007/978-3-319-17031-2_41.
[37] Haddad Djamel, Oulmi Kafia, Hocine Benmoussa ZA, Sahli Youcef. Modeling of Heat Transfer in the PEMFC: Velocity Inlet and Current Density Effect. In: Dincer I, Ozgur Colpan C, Kizilkan O, Akif Ezan M, editors. Progress in clean energy volume I: Analysis and Modeling. Switzerland: Springer; 2015. p. 463–73. 10.1007/978-3-319-16709-1_33.
[38] Mammar K, Chaker A. Flooding and drying diagnosis of proton exchange membrane fuel cells using electrochemical impedance spectroscopy analysis. J Electr Eng 2013;13:147–54.
[39] Danzer MA, Hofer EP. Analysis of the electrochemical behaviour of polymer electrolyte fuel cells using simple impedance models. J Power Sources 2009;190:25–33.
[40] Saadi A, Becherif M, Hissel D, Ramadan HS. Dynamic modeling and experimental analysis of PEMFCs: a comparative study. Int J Hydrogen Energy 2016;42:1544–57.
[41] Pérez-Page M, Pérez-Herranz V. Study of the electrochemical behaviour of a 300 W PEM fuel cell stack by Electrochemical Impedance Spectroscopy. Int J Hydrogen Energy 2014;39:4009–15.
[42] Fausett LV. Fundamentals of Neural Networks: Architectures, Algorithms, and Applications. Prentice-H 1994.
[43] Demuth H. Neural network toolbox. Networks 2002;24:1–8. https://doi.org/10.1016/j.neunet.2005.10.002.
[44] Taleb MA. Exploitation des mesures électriques en vue de la surveillance et du diagnostic en temps réel des piles à combustible pour application transport automobile. Thèse de doctorat, l'universite Paris-Saclay Preparee a Centralesupelec 2016. tel-01281328.